



Contents lists available at ScienceDirect

# Journal of Rock Mechanics and Geotechnical Engineering

journal homepage: [www.jrmge.cn](http://www.jrmge.cn)

## Full Length Article

# Coupling effect of pond ash and polypropylene fiber on strength and durability of expansive soil subgrades: An integrated experimental and machine learning approach

Nitin Tiwari, Neelima Satyam\*

Department of Civil Engineering, Indian Institute of Technology Indore, Indore, India

## ARTICLE INFO

### Article history:

Received 19 October 2020

Received in revised form

13 January 2021

Accepted 7 March 2021

Available online 1 May 2021

### Keywords:

Expansive soil subgrades

Waste utilization

Freezing-thawing (F-T)

Microstructural assessment

Pond ash (PA)

Polypropylene (PP) fiber

## ABSTRACT

This study explores the coupling effect of pond ash (PA) and polypropylene (PP) fiber to control the strength and durability of expansive soil. The PA is used to chemically treat the expansive soil and PP fiber is adopted as reinforcement against tensile cracking. The sustainable use of PA and PP fiber are demonstrated by performing mechanical (i.e. unconfined compressive strength, split tensile strength and ultrasonic pulse velocity), chemical (pH value, electrical conductivity and calcite content), and microstructural analyses before and after 2nd, 4th, 6th, 8th and 10th freezing-thawing (F-T) cycles. Three curing methods with 7 d, 14 d and 28 d curing periods are considered to reinforce the 5%, 10%, 15% and 20% PA-stabilized expansive soil with 0.25%, 0.5% and 1% PP fiber. In order to develop predictive models for mechanical and durability parameters, the experimental data are processed utilizing artificial neural network (ANN), in association with the leave-one-out cross-validation (LOOCV) as a resampling method and three different activation functions. The mechanical and durability properties of the PA-stabilized expansive soil subgrades are increased with PP fiber reinforcement. The results of ANN modeling predict the mechanical properties perfectly, and the correlation coefficient ( $R$ ) approaches up to 0.96.

© 2021 Institute of Rock and Soil Mechanics, Chinese Academy of Sciences. Production and hosting by Elsevier B.V. This is an open access article under the CC BY-NC-ND license (<http://creativecommons.org/licenses/by-nc-nd/4.0/>).

## 1. Introduction

The rapid development of the urban area and industrialization generates a shortage of useable land and soil conditions for civil engineering structures. The expansive soils are the most problematic soil types due to their nonrecurring swelling shrinkage nature and low bearing capacity (Puppala et al., 2017). The expansive soil in the foundation has an adverse impact on the performance of lightweight structures, especially in road pavement. Considering the geographical conditions of India, almost one-fifth of the land area is covered with expansive soils. Damage caused by expansive soil can be observed around the world, and the economic losses of approximately 7–9 billion US dollars per year have been reported in the United States alone (Steinberg, 1998). The layered structure of the clay minerals and cations adsorbed for the charged equilibrium induced swelling-shrinkage in expansive soil (Khazaei and Moayedi, 2019). Numerous remedies have been

successfully demonstrated to improve the engineering behaviors of the expansive soils, such as use of chemical alternation additives (Zhang et al., 2015; Moayedi and Nazir, 2018; Tataranni et al., 2018; Tiwari and Satyam, 2019), moisture control (Rojas et al., 2009), application of adequate surcharge pressure (Soundara and Robinson, 2009), biocementation (Sharma et al., 2019), biochemical treatment (Ikeagwuani and Nwonu, 2019; Liu et al., 2019), and geosynthetic inclusion (Singh et al., 2018; Tiwari and Satyam, 2020). The investigation on the improvement of expansive soil using the traditional stabilizer, i.e. lime and cement, are usually effective in improving the engineering properties of expansive soils (Camargo et al., 2013). Nonetheless, there are substantial problems for the long-term viability of these approaches, depending on soil clay mineralogy and ecological variations in clay (Ikeagwuani and Nwonu, 2019). The cement is the conventional chemical stabilizer that increases stability and durability (Al-Rawas et al., 2005), which causes global warming due to CO<sub>2</sub> emission (Wilberforce et al., 2019). The pond ash (PA) produced is generally neglected and discharged into the environment due to its porous and coarse-grained structure compared to fly ash (FA). The use of PA in civil engineering constructions can reduce the disposal problem, and

\* Corresponding author.

E-mail address: [neelima.satyam@iiti.ac.in](mailto:neelima.satyam@iiti.ac.in) (N. Satyam).

Peer review under responsibility of Institute of Rock and Soil Mechanics, Chinese Academy of Sciences.

the use of PA for subgrade soil stabilization has been effectively demonstrated (Bhurteel and Eisazadeh, 2020). Currently, less than 30% of the coal ash produced is reused, therefore, it is necessary to consider measures to improve its use. The chemical stabilization method is conventionally used to stabilize expansive soil and improve its compressive strength. However, it dispenses the slightest effect on the tensile strength. As a reinforcement measure, fibers could be used, e.g. nylon, polypropylene and coir (Tiwari et al., 2020a, 2021). The fiber reinforcement increased the shear strength of the reinforced materials and slightly improved the shear angle (Li et al., 2017). The reliability studies conducted by Moghal et al. (2018) reported the effect of synthetic fiber reinforcement on the CBR behavior of expansive soils mixed with lime. The study showed that fiber concentration and length have a significant influence on the CBR value. Chauhan et al. (2008) investigated the effectiveness of fiber reinforcement in the subsoil together with FA. The combined effect of bottom ash and fibers was studied by Prasannan et al. (2020) and showed the significant improvement of the hydro-mechanical properties of expansive soil subgrade. The curing method and duration have a significant influence on the strength of chemically treated soil with geopolymer material. Tiwari et al. (2020b) considered three different curing methods, i.e. moisture-controlled (MC), gunny bag (GB), and water-submerged (WS) curing for a period of 7 d, 14 d and 28 d, and presented the effect of curing period and method with silica fume and polypropylene fiber. Soil stabilization with chemical additives is useful in improving durability to withstand unfavorable environmental conditions such as freezing-thawing (F-T) (Behnood, 2018). Ding et al. (2020) reported that F-T cycles have an adverse impact on road pavement structures, and this damage occurs in the form of cracking, flaking of the surface layer and increased settlement in the subgrade. The damage caused by F-T cycles to subgrade soils can be attributed to the formation of ice lenses during freezing, which changes the soil structure at micro and macro-scales and reduces its integrity (Wong and Haug, 1991). Sudhakaran et al. (2018) studied the effect of bottom ash and areca fiber to improve the performance of the road pavement subgrade. However, the study did not present the long-term effect of the treatment. Areca fiber is a biodegradable and low-durability material, thus PP fiber was used to overcome the limitation of biodegradable fiber in this study.

The study aims to examine the coupling effect of PA and PP fiber on the strength and durability of expansive soil subgrades during F-T cycles. The quantification of the optimal proportion of PA and PP fiber was assessed by carrying out various mechanical, chemical and microstructural analyses. The effect of the three different curing methods at 7 d, 14 d and 28 d was considered to evaluate the effect of different curing methods and time periods on the treatment process. The various chemical and mechanical tests together with the microstructural analysis were carried out after multiple F-T cycles to understand the durability attributed to the expansive soil. The feasibility of fitting laboratory data to identify predictive equations of mechanical properties has already been successfully discussed by various researchers (Paykov and Hawley, 2015; Tizpa et al., 2015; Inkoomb et al., 2019). In such studies, large data sets are available, which are actually necessary for proper training of a neural model. Nevertheless, most of the time, the laboratory data set available is quite small, with respect to what is required by conventional neural approaches. In the present study, a nonconventional approach, i.e. the leave-one-out cross-validation (LOOCV), has been used to adequately train the neural network model based on the data set obtained by the experimental investigation in order to maximize the reliability of the artificial neural network (ANN) model despite the relatively few experimental data available.

## 2. Methodology

In this study, the detailed experiments and numerical analysis have been performed with varying percentages of the PP fiber and PA. A total of 408 samples were prepared for the detailed investigation.

### 2.1. Materials

The soil used in this study was collected at a depth of 2.5 m in the Indian Institute of Technology Indore campus, which is located in the state of Madhya Pradesh (India). The disturbed soil samples were obtained using a standard hydraulic excavator machine. The obtained soil samples were oven-dried, and their index properties were evaluated as per Indian Standards (IS 2720-1, 1983; IS 2720-3, 1980; IS 2720-4, 1985; IS 2720-5, 1985; IS 2720-7, 1980; IS 2720-40, 1977). The index properties of expansive soil are listed in Table 1. The soil is classified as highly plastic clay (CH) according to unified soil classification system (USCS) and shows a free swelling index of 120.

The PP fiber made of waste plastic was obtained from Bajaj Reinforcements (India). The dimensions of the fiber used for reinforcement is 12 mm in length and 18  $\mu$ m in diameter. The inert nature of the PP fiber with suitable moisture content makes it more durable. The higher tensile strength of the PP fiber shows effectiveness to reinforce the expansive soil. The properties of the PP fiber adopted in the study are shown in Table 2.

The cementation material used in this study is the non-combustible residue of coal known as PA. The chemical compositions and mechanical properties of PA are tabulated in Table 3. The material was collected from Satpura Thermal Power Station at Sarni (India). The disposal of the PA is a major concern of the thermal power authority. Its utilization in the paved structure construction can minimize the conventional chemical stabilizer like cement and lime and reduce its disposal problem.

**Table 1**  
Index properties of expansive soil.

Property	Value
Maximum dry unit weight ( $\text{kN/m}^3$ )	17.65
Optimum moisture content (%)	19.2
Liquid limit (%)	89
Plastic limit (%)	47
Plasticity index (%)	42
Shrinkage limit (%)	11
Composition (%)	Clay
	Silt
	Sand
Specific gravity	2.78
Free swelling index (%)	120
USCS soil classification	CH

**Table 2**  
Properties of PP fiber used in this study.

Property	Value
Strength (GPa)	0.67
Specific gravity	0.91
Length (mm)	12
Diameter ( $\mu$ m)	18
Aspect ratio	667
Modulus of elasticity (GPa)	4
Melting temperature ( $^{\circ}\text{C}$ )	165
Ignition temperature ( $^{\circ}\text{C}$ )	600
Bulk density ( $\text{kg/m}^3$ )	910
Loosen density ( $\text{kg/m}^3$ )	250–430
Salt and acid effect	Excellent

**Table 3**

Properties of PA used in this study.

Property	Value
Specific gravity	2.43
Dry unit weight (kN/m <sup>3</sup> )	7.68
Plasticity	–
Chemical composition (%)	
SiO <sub>2</sub>	52.68
SO <sub>3</sub>	0.24
Al <sub>2</sub> O <sub>3</sub>	21.52
Fe <sub>2</sub> O <sub>3</sub>	20.37
CaO	1.17
TiO <sub>2</sub>	1.1
K <sub>2</sub> O	2.08
MgO	0.23
Na <sub>2</sub> O	0.21
P <sub>2</sub> O <sub>5</sub>	0.32
Loss on ignition	0.08

## 2.2. Sample preparation

The collected soil samples were air-dried for 24 h and then oven-dried for another 24 h at 105 °C. The test samples were prepared with 5%, 10%, 15% and 20% PA and 0.25%, 0.5% and 1% PP fiber in different combinations. The test samples were prepared to evaluate the effect of PA and PP as an individual along with its coupling effect on expansive soil subgrades. The soil, PP fiber and PA mixture was prepared at optimum moisture content and placed in the environmental chamber at temperature of (27 ± 2) °C and humidity of 65% ± 5% for compacting the sample into the desired shape. All the mixing proportions with different test parameters are tabulated in Table 4.

A total of 408 cylindrical samples (38 ± 2 mm in diameter and 76 ± 4 mm in length) were prepared and placed for 7 d, 14 d and 28 d of curing. Three different curing methods, i.e. MC, GB, and WS, were used to understand the curing effect. In MC curing, the prepared samples were placed in the environmental chamber at (20 ± 2) °C and 100% ± 5% humidity. The compacted samples were warped with the aluminum foil and placed in the environmental chamber. The environmental chamber was configured according to the Indian standard requirements for curing (IS 2720-1, 1983).

In contrast, in WS curing, the samples were packed in the thin membrane and then submerged in the water tank at room

temperature (27 ± 2 °C). The glass water tank was used to avoid any contamination in the water with metal. The water level of 50 mm above samples has been continuously maintained. In GB curing, the samples were directly warped in the wet GB, and water was sprinkled in every 6 h to keep the constant moisture content.

All the samples were grouped into three categories for three different curing methods, and each group of samples was divided into three equal parts for 7 d, 14 d and 28 d of curing. For each test, three replicas have been prepared to understand the reproducibility of the test results.

## 2.3. Chemical and microstructural analysis

The stabilization of expansive soil with PA resulted in change of chemical and microstructural arrangements of soil structure. The quantification of the chemical alternation by adding PA in the expansive soil with different curing methods and periods, pH value, electrical conductivity (EC), and calcite content (CCt) was performed on each sample. The CCt formation is the direct reflection of the hydration reaction of the PA. Therefore, to quantify the effect of the different curing methods on hydration, the CCt was calculated. The EC and pH value can signify the change in the chemical state of the expansive soil with PA. The mineralogical characterization using XRD was carried out on all the treated samples with varying PA contents. The XRD test was performed on a powder sample. Similarly, to understand the change in chemical bonds during the treatment process, attenuated total reflection-Fourier-transform infrared (ATR-FTIR) analysis was carried out on potassium bromide (KBr) pellet samples. The FTIR scans were made from 400 cm<sup>-1</sup> to 4000 cm<sup>-1</sup> using the ATR-FTIR spectrometer (PerkinElmer). In all the aforementioned chemical and mineralogical analyses, only the effect of the PA content was analyzed since the inert change of the PP fiber has no influence on the chemical properties of the treated expansive soil. The coupling effect of the PP fiber with PA on soil matrix at microstructure was studied using scanning electron microscopy (SEM). The elements were identified by performing energy dispersive X-ray (EDX) analysis. The freezing-cut-drying method was used to prepare the sample for SEM and EDX since this method preserves the original microstructure (Shi et al., 1999).

## 2.4. Mechanical properties analysis

The strength and durability of the treated and untreated samples were assessed by carrying out unconfined compressive strength (UCS), split tensile strength (STS), and ultrasonic pulse velocity (UPV) tests before and after F-T cycles. The initial strengths of all samples were assessed, and then the samples were placed in the F-T chamber for durability assessment. The closed chamber of the F-T was configured to the temperature variation from –20 °C to 20 °C (Lu et al., 2016). Ten cycles of 12-h freezing and 12-h thawing were carried out. After the 10th cycle, expansive soil reflects constant deformation (Lu et al., 2019). The effect of F-T on each group of samples was assessed by UCS, STS, and UPV after 2nd, 4th, 6th, 8th, and 10th cycles, respectively. The mechanical property tests were conducted according to Indian Standards (IS 2720-10, 1991; IS 10082, 1981), and the average value of the three replicas are presented in the results.

## 2.5. Machine learning approach using ANN

The machine learning approach was used to predict the mechanical performances of the recycled ash and synthetic fiber stabilized expansive soil subgrades. ANN tool of machine learning was considered in this study. The ANN models are developed using

**Table 4**

Experimental test program.

Sample ID	Material percentage (% by weight)			Test performed	Number of samples
	BC	PA	PP		
BC	100	0	0	UCS, STS, UPV, CP	24
BC+5%PA	95	5	0	UCS, STS, UPV, CP	24
BC+5%PA+0.25%PP	94.75	5	0.25	UCS, STS, UPV	24
BC+5%PA+0.5%PP	94.5	5	0.5	UCS, STS, UPV	24
BC+5%PA+1%PP	94	5	1	UCS, STS, UPV	24
BC+10%PA	90	10	0	UCS, STS, UPV, CP	24
BC+10%PA+0.25%PP	89.75	10	0.25	UCS, STS, UPV	24
BC+10%PA+0.5%PP	89.5	10	0.5	UCS, STS, UPV	24
BC+10%PA+1%PP	89	10	1	UCS, STS, UPV	24
BC+15%PA	85	15	0	UCS, STS, UPV, CP	24
BC+15%PA+0.25%PP	84.75	15	0.25	UCS, STS, UPV	24
BC+15%PA+0.5%PP	84.5	15	0.5	UCS, STS, UPV	24
BC+15%PA+1%PP	84	15	1	UCS, STS, UPV	24
BC+20%PA	80	20	0	UCS, STS, UPV, CP	24
BC+20%PA+0.25%PP	79.75	20	0.25	UCS, STS, UPV	24
BC+20%PA+0.5%PP	79.5	20	0.5	UCS, STS, UPV	24
BC+20%PA+1%PP	79	20	1	UCS, STS, UPV	24

Note: BC - black cotton; UCS - unconfined compressive strength; STS - split tensile strength; UPV - ultrasonic pulse velocity; CP - Chemical Properties.

weighted and biased correlations of logistic regression, which is called artificial neurons. The networks are built up in three components, i.e. input layer, hidden layers, and output layer. The input layer neurons are used to obtain the details of the various parameters and hidden layers to develop the correlation between them to create the output network. A prediction of the output network is made based on the weighted and biased correlations of input parameters. The nonlinear activation function controls the training of each neuron. ANN models are used to develop the correlation between input parameters and target output. Supervised training of neurons is carried out to minimize the error in the predicted and experimental results.

In this research, shallow neural networks (SNNs) were considered to predict the mechanical performances of stabilized expansive soil. The model is capable of developing strong correlations between multidimensional input parameters and targeted output. To minimize the error in the predicted results, sufficient neurons were assigned in the hidden layer during training. The SNN models used in this study consisted of a 5-neuron input layer and 3-neuron output layer. The nonlinear activation function in the hidden layer was applied to develop the correlations between the 7-neuron input layer and 3-neuron output layer, which is the grid search approach for the characterization of the number of neurons  $N$  and mathematical nonlinear activation function. The combination of the number of neurons and activation function, which yields the lowest score to prediction error, was used. The unit activation functions including logistic sigmoid (LogS), the exponential linear (ELU), and the rectified linear (ReLU) (Fig. 1) were applied to find the optimum prediction model. The integer range  $X_N = \{1, 2, \dots, 100\}$  were considered for finding the neurons in hidden layer.

Five input parameters such as PA content, PP fiber content as well as the categorical parameters that distinguish curing methods (values: MC = 0, GB = 1 and WS = 2), curing period (values: 7 d = 7, 14 d = 14 and 28 d = 28), and F-T cycles (values: 0, 2, 4, 6, 8 and 10) were taken into account for developing the correlation to predict the targeted experimental results. UCS, STS and UPV of stabilized and unstabilized expansive soil subgrades were considered as output parameters. All the parameters were rescaled to have a unit standard deviation and a zero mean to minimize the computation time and increase the efficiency of SNN model.

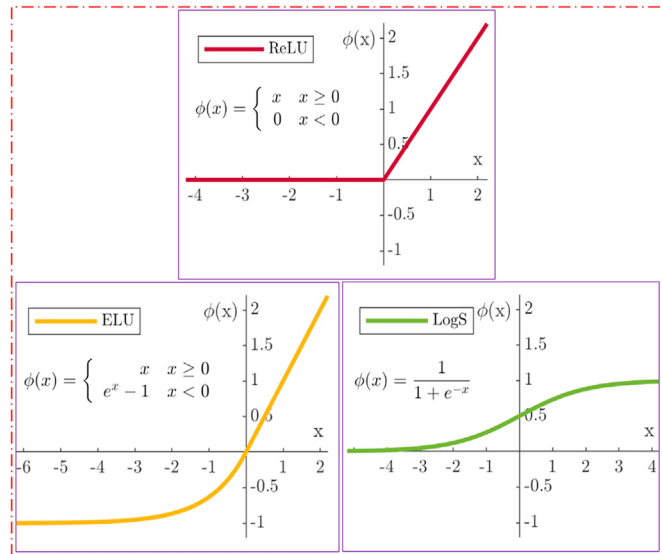


Fig. 1. Activation functions of exponential linear (ELU), rectified linear (ReLU), and logistic sigmoid (LogS).

## 2.6. ANN training and regularization

The supervised training is used to reduce the prediction error between the ANN output  $\hat{y}$  and the experimental target  $y$  with respect to the input parameters  $x$ . The process is carried out to develop close correlations between the input parameters and target output. The weights and biases for each input have been calculated during the training of the model. The training process is carried out in two phases, i.e. forward and backward passes. The neurons are trained with the application of several mathematical nonlinear activation functions to obtain the output  $\hat{y}$  using input parameter vector  $x$  during the forward stage. After that, a backward stage is applied to compute the loss function. During this stage, a comparative analysis is carried out between the computed output  $\hat{y}$  and the experimental target vector  $y$  using performance function  $F(\hat{y}, y)$ . The correlation of the weights and biases of the SNN are computed in the backward stage. The training and regulation process includes the application of the learning rule to compute the network parameters  $W$  (matrix of weights and biases). The network parameters are computed as per assumed values of a performance function for a fixed number of iterations  $E$ . The mean square error (MSE) is computed using the backpropagation algorithm in learning rules. MSE is used to update the network parameters by minimizing the loss values. The MSE is accepted as  $F(\cdot)$  function and its gradient with respect to  $W$ . The analytical expression used for training and regulation of the SNN model is written as

$$W^{e+1} = W^e - [\nabla^2 F(W^e)]^{-1} \nabla F(W^e) \quad (e \in \{1, 2, \dots, E\}) \quad (1)$$

The Levenberg-Marquardt (LM) backpropagation algorithm used are written as

$$W^{e+1} = W^e - [J^T(W^e)J(W^e) + \mu_e I]^{-1} J^T(W^e) v(W^e) \quad (e \in \{1, 2, \dots, E\}) \quad (2)$$

where  $W^e$  is the matrix of weights and biases at iteration  $e$ ,  $J$  is the Jacobian matrix of the training loss  $F(\cdot)$  with respect to  $W^e$ ,  $I$  is the identity matrix,  $v(W^e) = \hat{y}(W^e) - y$  is the vector of network errors, and  $W^{e+1}$  is the updated values of network parameters to be used in the forward stage of iteration  $e + 1$ . The direction towards the minimum is determined by the gradient  $J^T(W^e)v(W^e)$ , and the scalar  $\mu$  determines the step size taken in that direction at each iteration. In particular, a high  $\mu$  value corresponds to a small learning step and a very long convergence time. On the contrary, a low  $\mu$  allows the convergence speed to increase, but the algorithm could jump over the minimum. In order to achieve faster convergence and in parallel avoid undesirable local minima, the parameter  $\mu$  is varied during training: the value  $\mu_{e+1}$  corresponds to  $\mu_e$  multiplied by  $\mu_{inc} > 1$  (or  $\mu_{dec} < 1$ ) if the performance index has increased (or decreased) between iterations  $e - 1$  and  $e$ . In addition, if the parameter  $\mu$  becomes too large, i.e.  $\mu_{e+1} > \mu_{max}$ , the LM algorithm is terminated.

The true conversion of the model is expressed if the maximum value of  $\mu$  is reached during training. The optimal values of the weights and biases are obtained after the end of iterations. The model's loss index on novel data is computed by processing the feature vector in a forward manner, whereas the fix values of weights and biases are used. The higher value of the weights increases the slope of a network activation function. The increase in the slope of network function may cause the overfit of training data. The regularization methods are used to control the overfit of the training data and increase the model's performance score. The



method is applied to smooth the resulting activation function and penalize network complexity. During the regularization process, the MSE is modified by including the term sum of squares of the network weights. Therefore, the ANN model is optimized by

$$F_{\text{opt}}(\hat{\mathbf{y}}(\mathbf{W}^e), \mathbf{y}, \mathbf{W}^e) = \beta \|\hat{\mathbf{y}}(\mathbf{W}^e) - \mathbf{y}\|_2^2 + \alpha \|\mathbf{W}^e\|_2^2 \quad (3)$$

where the operator  $\|\cdot\|_2^2$  represents the 2-norm, applied to the network's parameters  $\mathbf{W}^e$  and errors  $\mathbf{v}(\mathbf{W}^e) = \hat{\mathbf{y}}(\mathbf{W}^e) - \mathbf{y}$ ; and  $\alpha$  and  $\beta$  are the regularization parameters that control the complexity of the network solution: the ratio  $\alpha/\beta$  assumes values in the interval  $[0, 1]$ .

The smooth ANN response is obtained with the increasing value of the ratio  $\alpha/\beta$ . The higher value of the ratio  $\alpha/\beta$  creates an overly smooth interpolation of the ANN model. While lower values of the ratio  $\alpha/\beta$  causes the network to be overfitted for the data. Therefore, optimization of ratio  $\alpha/\beta$  is the critical parameter to be considered during the regularization process.

David MacKay's approach has been used to optimize the regularization parameters (MacKay 1992). This approach uses Bayesian statistics to train ANN model. With the application of David MacKay's approach,  $\alpha$  and  $\beta$  were re-computed after every iteration.

MATLAB® ANN Toolbox has been used to implement the ANN model for predicting the experimental results. The hyper-parameters of LM algorithm ( $\mu$ ,  $\mu_{\text{inc}}$ ,  $\mu_{\text{dec}}$ ,  $\mu_{\text{max}}$  and  $E$ ) have been kept at their default values. The maximum number of training epochs  $E$  is set to 1000,  $\mu_{\text{dec}}$  to 0.1,  $\mu_{\text{inc}}$  to 10, the highest  $\mu$  value that stops training is  $1 \times 10^{10}$ , and the initial  $\mu$  is 0.001.

## 2.7. LOOCV

In general, in order to perform the ANN analysis, the available data set was randomly divided into two categories, i.e. the training data set and the test data set. This process of distributing the data set for training and testing is known as the hold-out method. Since the data set is randomly divided, it can give a biased model to predict the target output. The model error will increase based on

the missing trends in the training data set and the test data set. There is also a risk of missing out on the important training trend due to the biased distribution of the data. In the case of a small dataset for training and testing, this error will be higher. To avoid this, LOOCV method is used to train the ANN model. As shown in Fig. 2, in the LOOCV method, the partitioning of the experimental data set into a training data set is performed by dividing the data set into several steps. In each step, a completed data set is used for training except one data set, which will be considered for test observation.

The ANN model trained by the LOOCV method for the  $n - 1$  observations and obtained the best model to predict the excluded data set. This split process to separate data is performed for  $n$  splits. Each time the test data set is changed, and another completed data set is considered for testing. During each split data set, MSE values are calculated. The MSE is calculated as the squared difference between the prediction  $\hat{y}_i$  and the experimental value  $y_i$  of the excluded observation:  $MSE_i = \|\hat{y}_i - y_i\|_2^2$ . The test error of the ANN model is then estimated by taking the average of the  $n$  resulting mean squared error:

$$MSE_{\text{CV}} = \frac{1}{n} \sum_{i=1}^n MSE_i \quad (4)$$

Hence, the LOOCV method trains the ANN model on an approximately complete data set. This method is highly useful for a particularly small data set. Since the complete data set is used for the training, the model is highly unbiased, and the prediction error is low. The LOOCV method also minimizes the error that occurred during the hold-out splits method.

Nevertheless, the model presented in this study aims to describe the mechanical properties of expansive soil subgrades stabilized with PA and PP fiber. For this reason, cross-validation was implemented by excluding one observation for each input parameter. In this way, it is possible to reduce the computational cost of the fitting models and to decrease the variance of the cross-validation procedure because the overlap between the training sets is lower, and therefore, the model outputs are somewhat less correlated to each other.

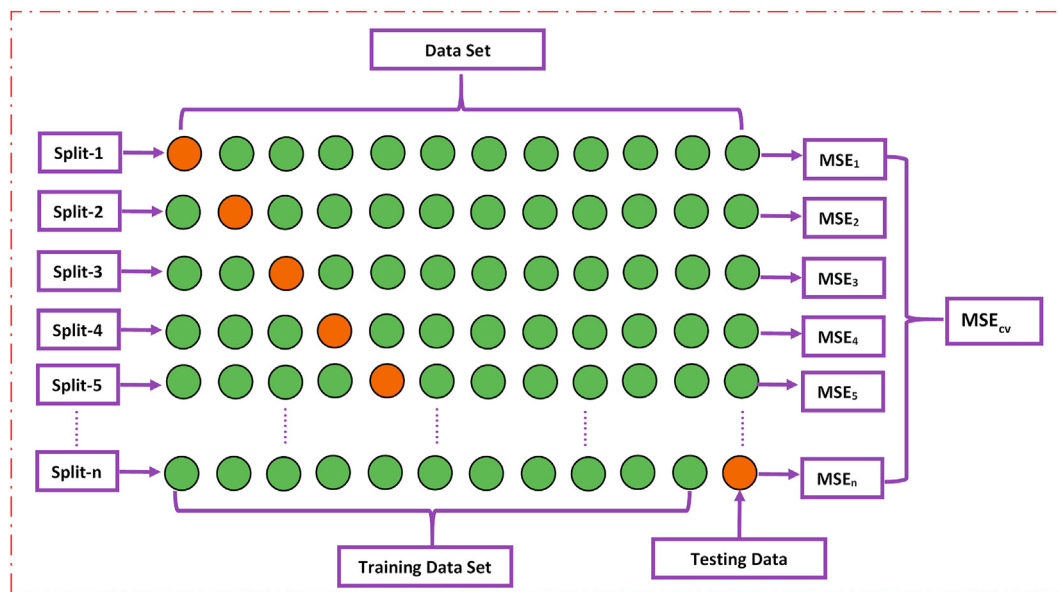


Fig. 2. Schematic representation of the LOOCV procedure.

### 3. Results and discussion

The expansive soil collected from the Indian Institute of Technology Indore campus located in Madhya Pradesh (India) was stabilized with PA and PP fiber. The effect of three curing methods, three curing periods, and different F-T cycles was considered to study the performances of stabilized expansive soil subgrades. A detailed discussion of the experimental and predicted results of machine learning model are presented in this section.

#### 3.1. Effect of curing method and period on UCS

The UCS values of the expansive soil with varying percentages of the PA and PP fiber contents are shown in Fig. 3. The effect of three different curing methods on the UCS value of the treated expansive soil with 7 d, 14 d and 28 d curing periods was analyzed. The surface polynomial curve fitting was analyzed to understand the effect of different curing methods with varying curing periods. The UCS value of treated expansive soil with increasing PA content was increased.

An increase in strength with the addition of PA content can be ascertained due to the polymerization process. During the curing process, the hydration reaction takes place, and as a result, calcium silicate hydrate (CSH) is formed. The CSH gel formation produced a strong soil PA matrix, and an increment in the UCS was observed. With the increasing curing period, more hydration gel increased, and it is clearly observed that 28 d of cured samples show higher strength than the 14-d and 7-d cured samples. The effect of PP fiber on UCS is minimal, and a very slight improvement has been observed. The reinforcement with the PP fiber increases interfacial mechanical interactions. However, higher PP fiber content reduced the binding between soil particles, and a reduction in the UCS was observed at 1% PP fiber. It is confirmed that the polynomial surface curve for the WS curing is the highest in all the curing periods, which proves that the WS curing is highly effective for the curing

method. Although the MC curing effect is almost similar to the WS curing, however, the GB cured samples have the least UCS.

#### 3.2. Effect of curing method and period on pH, CCt and EC

The chemical alternations with the varying contents of the PA are presented in Fig. 4. The EC values are presented on the primary Y-axis and pH and CCt on the secondary Y-axis. The value of EC is increased with the increasing percentages of PA. The increase in EC values depicts the chemical alternation in the soil-PA mixture. During the hydration process, the temperature of the soil-PA mixture was increased, which subsequently increased the EC (Bouziadi et al., 2016). The pH of the soil-PA mixture was raised, and it depicts the change in the nature of the mixture toward alkaline nature. The study shows that the increase in the pH values results in the increasing shear strength of soil (Goodarzi et al., 2016). The

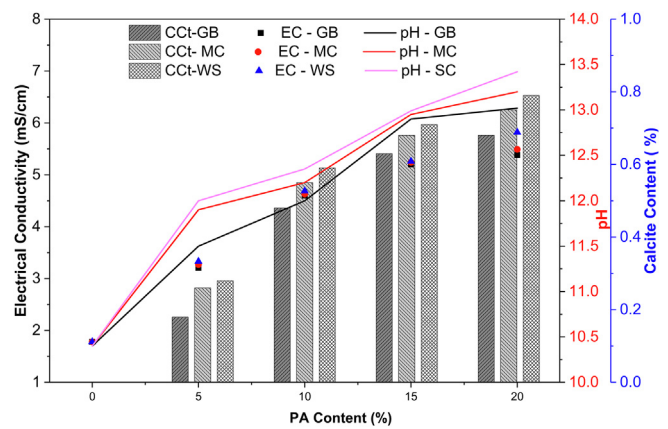


Fig. 4. Effect of bottom ash on EC, pH and CCt.

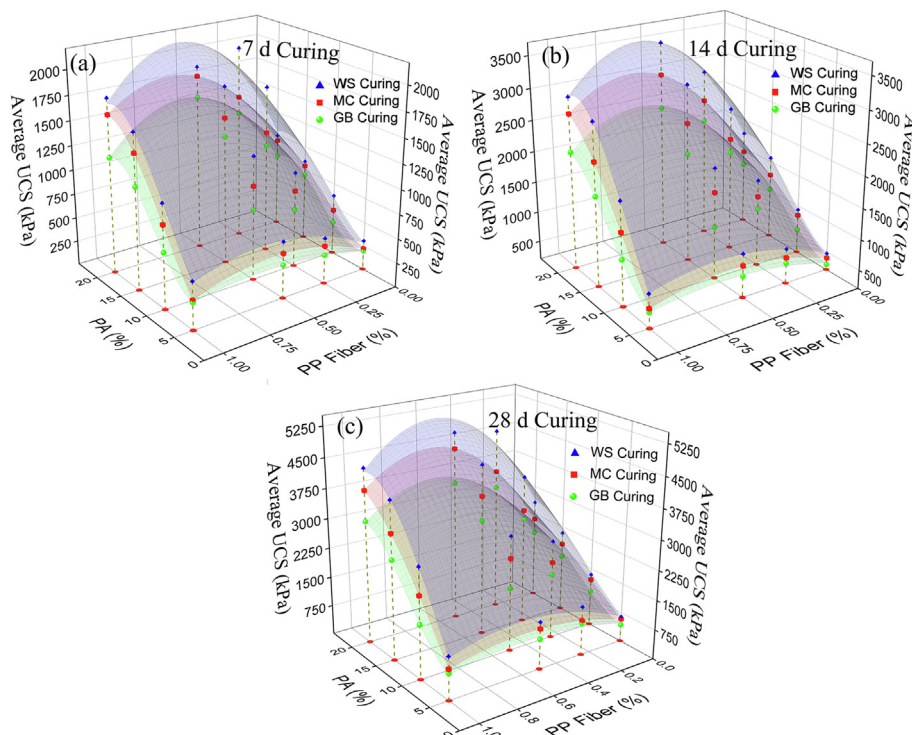


Fig. 3. Effect of curing method and period on UCS.

hydration creation formed a CSH gel that produced CCT in the mixture. The CCT test has been conducted to quantify the percentage of the calcite in treated samples. The CCT has been increased by up to 6.5% with the addition of the 20% PA content. A similar trend of the curing method has been observed at UCS. The WS curing shows more effective results than the GB and MC curing.

### 3.3. Effect of curing method and period on chemical bonds

The FTIR analysis has been performed on the varying PA content with different curing methods (Fig. 5). The FTIR spectra of each curing method has been compared with varying percentages of the PA content, i.e. 5%, 10%, 15% and 20%. The Infrared radiation (IR) range of 500–1200  $\text{cm}^{-1}$  shows the mineral, 1200–3000  $\text{cm}^{-1}$  shows the organic matters, and 3500–4000  $\text{cm}^{-1}$  shows the clay minerals (Tiwari et al., 2020c). The hydroxyl group of kaolinite and illite is observed in the IR band of 3092–3717  $\text{cm}^{-1}$ . The presence of the moisture content is observed at 3433  $\text{cm}^{-1}$ . A broad IR peak has been observed at the 3454  $\text{cm}^{-1}$ , showing the presence of CSH gel formation in the treated sample (Sharma et al., 2018). An intensified peak is observed with 20% PA content, which shows a higher amount of CSH gel formation with a higher content of PA. The broad IR band is observed due to free dissolved calcium (Ca), which offers nucleation for geopolymerization (Temuujin et al., 2009). A very narrow IR band is observed in the GB cured samples, which signifies the less hydration reaction during GB curing. A C–O bond peak has been observed at 874  $\text{cm}^{-1}$  and 1468  $\text{cm}^{-1}$ .

The increasing content of PA reduced the C–O bond peak, which ascertained the reduction in the carbonate (García-Lodeiro et al., 2010). The division in carbonation peak was obtained at 1430–1468  $\text{cm}^{-1}$  due to the partial carbonation of the hydration product (Kalinkin et al., 2004). The presence of the quartz was obtained at the IR peak of 798  $\text{cm}^{-1}$  and 782  $\text{cm}^{-1}$ . The IR peak observed at 3623  $\text{cm}^{-1}$  ascertained montmorillonite in the untreated BC soil. This peak has been reduced with the increasing PA content. This

shows that the addition of the PA content controls the presence of hydrophobic minerals (Tiwari et al., 2020d).

### 3.4. Effect of curing method and period on mineralogy

The mineralogical changes due to the addition of PA in the expansive soil after WS, MC and GB curing for 7 d, 14 d and 28 d were analyzed using X-ray diffraction (XRD) (Fig. 6). The formation of the CSH gel and portlandite was observed in XRD pattern.

In all samples, quartz has a highly distinct peak. It is evident that due to the formation of CSH gel, the presence of the tobermorite mineral should be observed. The XRD pattern shows the sharp peak of the tobermorite mineral in WS cured samples, which shows that the higher hydration gel is produced in the WS curing with 28 d period. The reduction in the peak of quartz was observed, which shows the utilization of minerals in geopolymerization action. An almost similar trend was observed with the MC curing method. However, the low intensity of tobermorite in GB shows the minimal effect of hydration in this method.

### 3.5. Effect of PA content on the chemical element formation in BC soil

The EDX of the selective SEM was carried out to confirm the presence of the chemical elements (Figs. 7 and 8). The EDX spectra for WS cured samples with 5%, 10%, 15% and 20% PA content were obtained. Due to the formation of CSH gel, a intensify peak of Ca was observed in all samples.

The higher Si content is also observed, which ascertained the presence of the quartz. The peak of Ca and Al is also observed, which gives favorable conditions for the formation of hydration gel. The presence of Ca and Al confirms the appearance of the aluminosilicate gel or calcium silicate gel in the treated expansive soil (Bilondi et al., 2018). The higher amount was observed with 20% PA content, which reflects the higher formation of the CSH or CASH gel

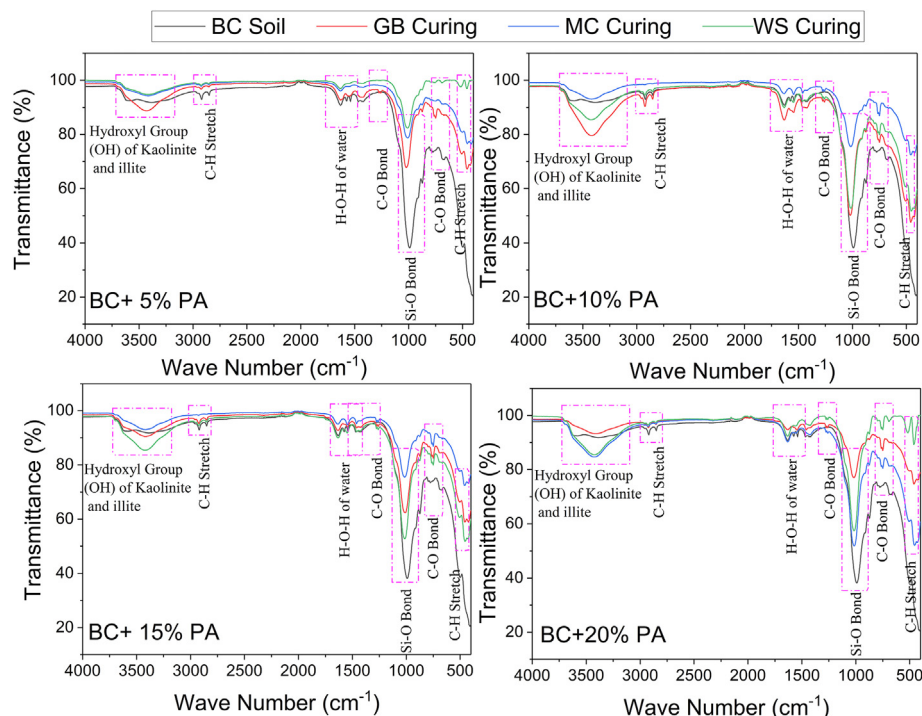
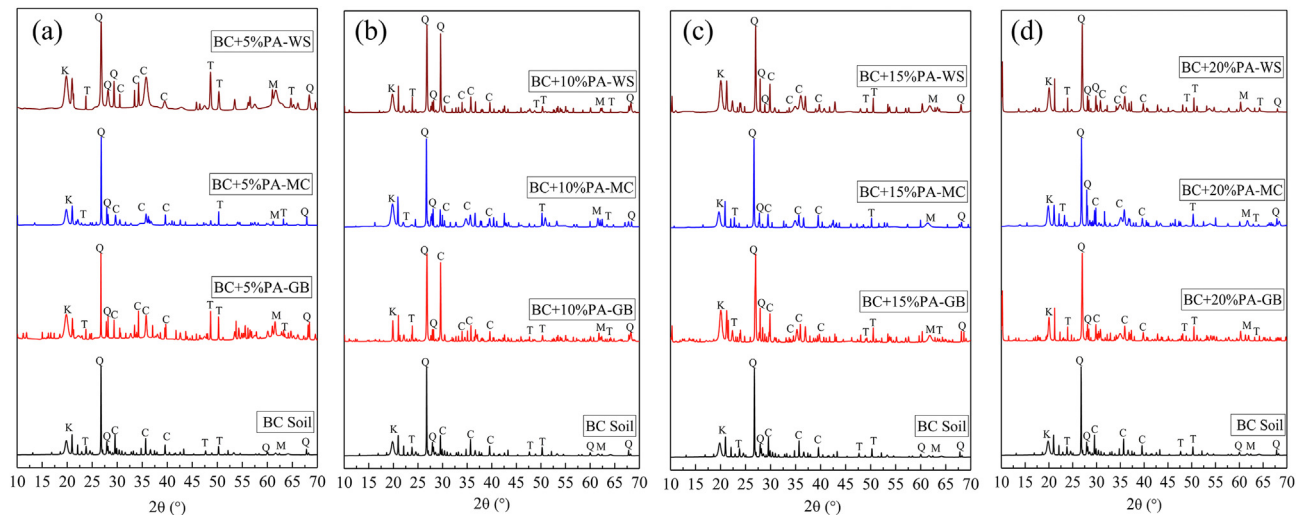
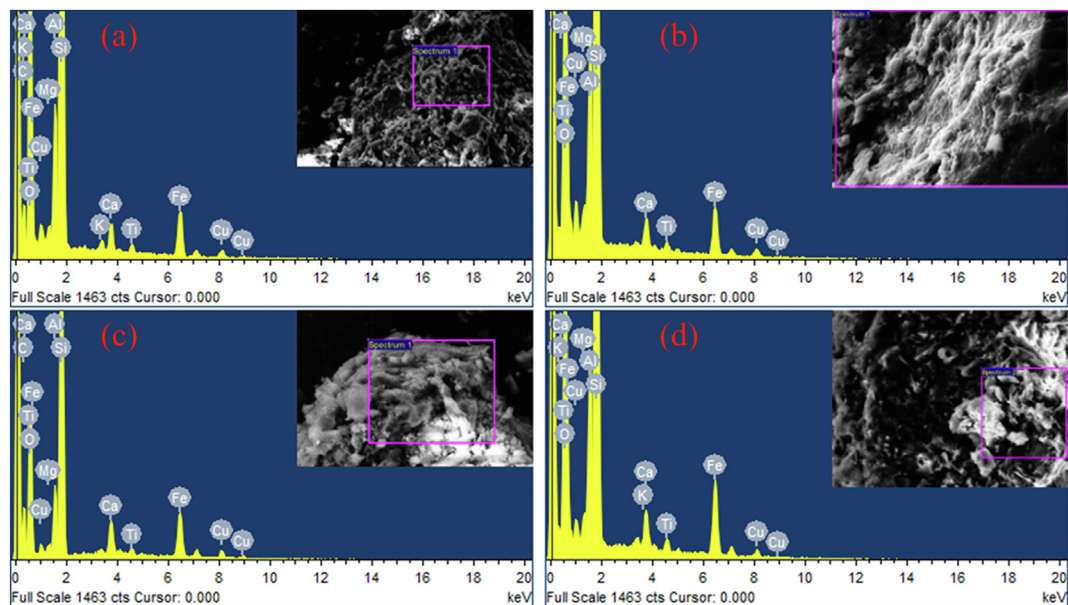


Fig. 5. FTIR spectra of the effect of the curing method on treated and untreated expansive soils.





**Fig. 6.** XRD spectra of the effect of the curing methods on treated and untreated expansive soils: (a) 5% PA, (b) 10% PA, (c) 15% PA, and (d) 20% PA. K - kaolinite; T - tobermorite; Q - quartz; C - calcite; M - Montmorillonite.



**Fig. 7.** EDX spectra of the effect of the curing method on (a) untreated expansive soil, (b) 20% PA treated expansive soil, (c) 15% PA treated expansive soil, and (d) 10% PA treated expansive soil.

in the treated samples. The XRD and FTIR results also confirmed the obtained elements in the EDX. The higher concentration of Si peaks is favorable for increasing the UCS value (Canakci et al., 2019).

### 3.6. Effect of curing method on UCS and UPV under F-T cycle

The UPV and UCS of the PA stabilized and PP fiber-reinforced expansive soil under F-T cycles were evaluated (Figs. 9 and 10). It was observed that the durability of the treated sample depends on its UCS and UPV retained capacity.

The UCS and UPV values were recorded after every even cycle of F-T (i.e. 2, 4, 6, 8 and 10) to assess the durability of treated samples. It was observed the UCS and UPV was increased with a higher concentration of PA (Fig. 3). The strength and stiffness of the PA-treated samples were increased due to the formation of a stable spatial network structure (Lu et al., 2019). However, during F-T cycles, the samples underwent the nonrecurring volumetric

change, and as a result, the bond of CSH gel broke, and reduction in the strength was observed with increasing F-T cycle. It was clearly observed that the lower concentration of PA content produced less CSH gel, and subsequently, a higher strength loss was reported. As mentioned above, the WS curing produced higher hydration gel and sound sample, therefore, higher UCS and UPV values were both observed compared with the MC and GB curing. Although MC curing had almost similar behavior as observed in the WS cured samples, a higher concentration of the CSH gel produced a strong soil-PP fiber matrix, which further showed a lower loss in the UCS and UPV during the F-T cycles.

### 3.7. Effect of curing method on STS under F-T cycle

The increase in UCS was observed with the addition of PA. However, addition of PA also increased the brittle nature in the treated samples. An STS test was carried out to assess the treatment effect of



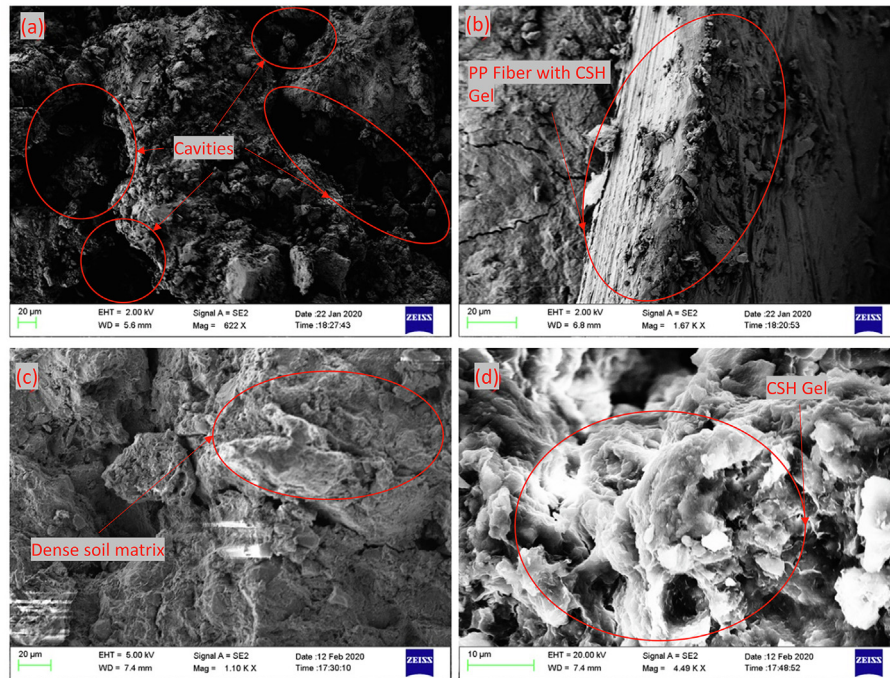


Fig. 8. SEM micrograph of (a) untreated expansive soil, (b) coupled effect of PP fiber and PA, (c) PA stabilized expansive soil, and (d) formation of CSH gel with PA stabilization.

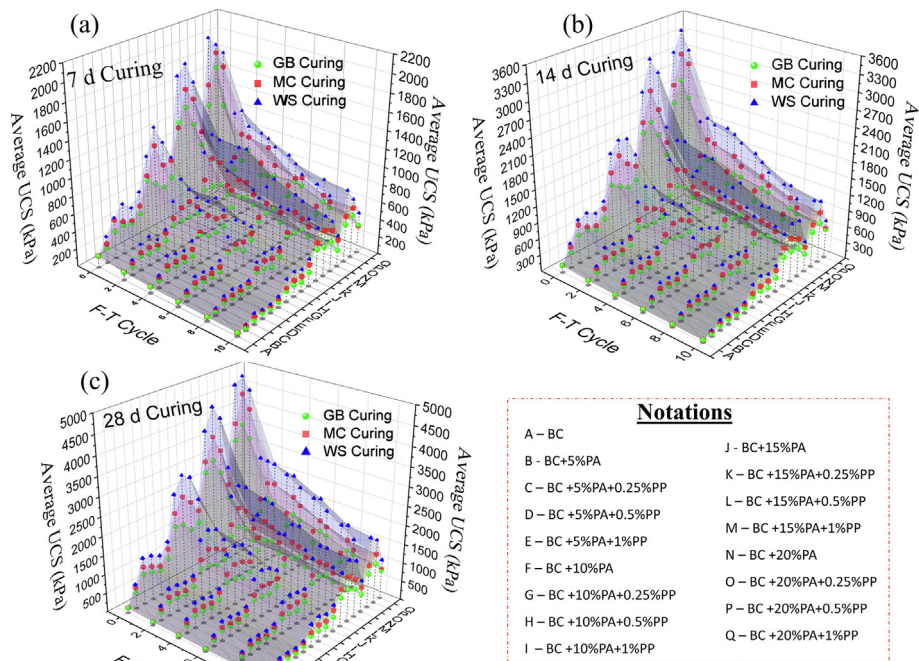


Fig. 9. Effect of curing method on UCS of treated and untreated BC soils under F-T cycle: (a) 7 d, (b) 14 d, and (c) 28 d.

PA and PP fiber on expansive soil. All the treated samples before and after F-T cycles were tested for the STS to explore the effect on tensile cracking mitigation in expansive soil (Fig. 11). The PP fiber increased the interfacial interaction between the soil particles, which further increased the tensile strength in the expansive soil. The PP-reinforced expansive soil subgrade showed higher tensile strength.

The tensile strength up to 0.5%PP fiber was increased. However, further addition of the PP fiber reduced the bond between soil particles and tensile strength. It was also observed that after the 6th

F-T cycle, the untreated expansive soil failed, hence, the STS value was reported as zero. Since the PP fiber is inert in temperature variation, a very minimal effect of F-T was observed with PP fiber-reinforced samples and retained the maximum strength. However, due to the fact that nonrecurring swelling-shrinkage behavior during the F-T cycles could break the CSH gel bond, the reduction in STS was observed with the increasing F-T cycles (Du et al., 2019). The higher strength was observed with 20% PA and 0.5% PP fiber content.

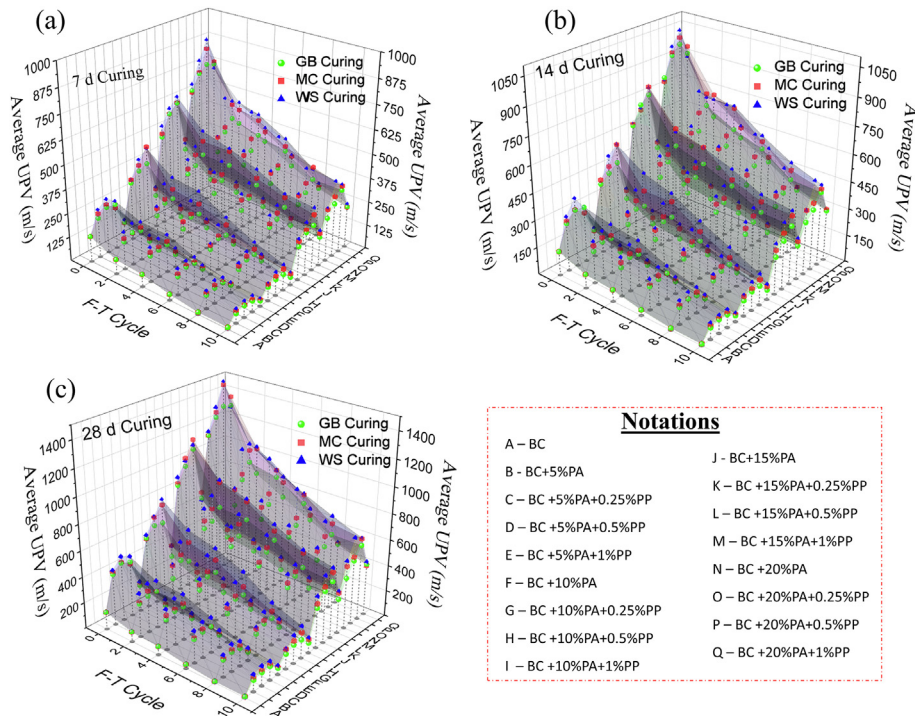


Fig. 10. Effect of curing method on UPV of treated and untreated BC soils under F-T cycle: (a) 7 d, (b) 14 d, and (c) 28 d.

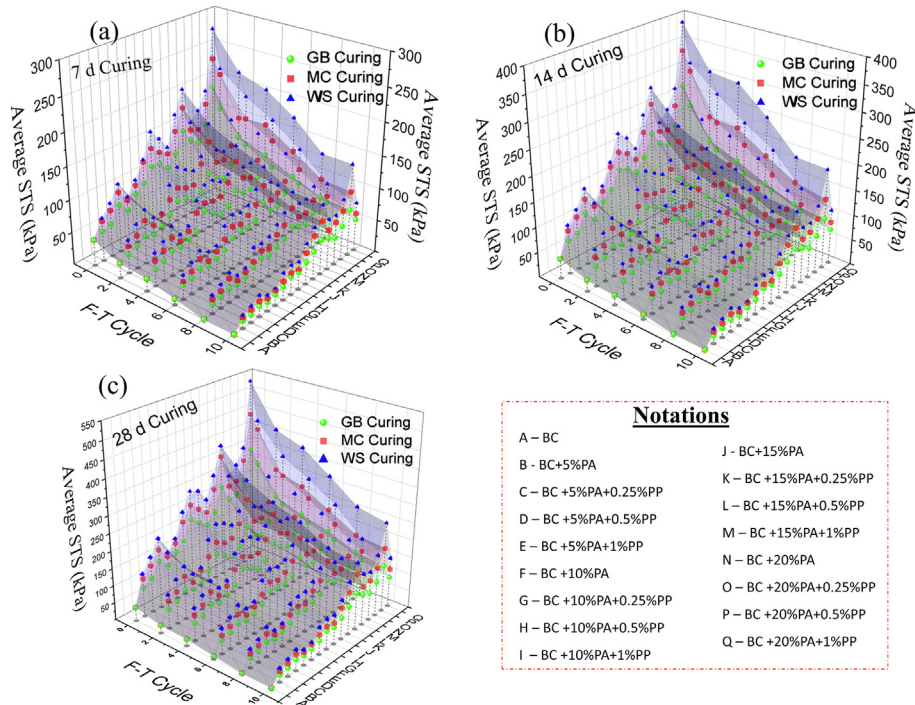


Fig. 11. Effect of curing method on STS of treated and untreated BC soils under F-T cycle: (a) 7 d, (b) 14 d, and (c) 28 d.

### 3.8. Prediction of the mechanical properties using ANN model

The smooth and accurate regression model with small data set is obtained by applying the LOOCV approach for sampling into the SNN training and testing of the data set. As shown in Fig. 12, the grid search approach gives ease in finding an optimum model. The ELU activation function with 8 neurons in the hidden layer gives  $MSE_{CV}$  of 0.09393 and a correlation coefficient ( $R$ ) of

0.95052. The model is referred to as ELU-SNN model for ANN, whereas SNN-LogS model gives a slightly better output. It can be observed that in SNN-LogS model, the  $MSE_{CV}$  equals 0.09021, and the correlation coefficient ( $R$ ) is 0.95184. The SNN-LogS model is characterized by 6 neurons. However, the SNN-ReLU model is characterized by 29 neurons in a hidden layer with  $MSE_{CV}$  of 0.15144, and the correlation coefficient ( $R$ ) of 0.91788. Higher value of  $MSE_{CV}$  and lower value of  $R$  show the poor performance of



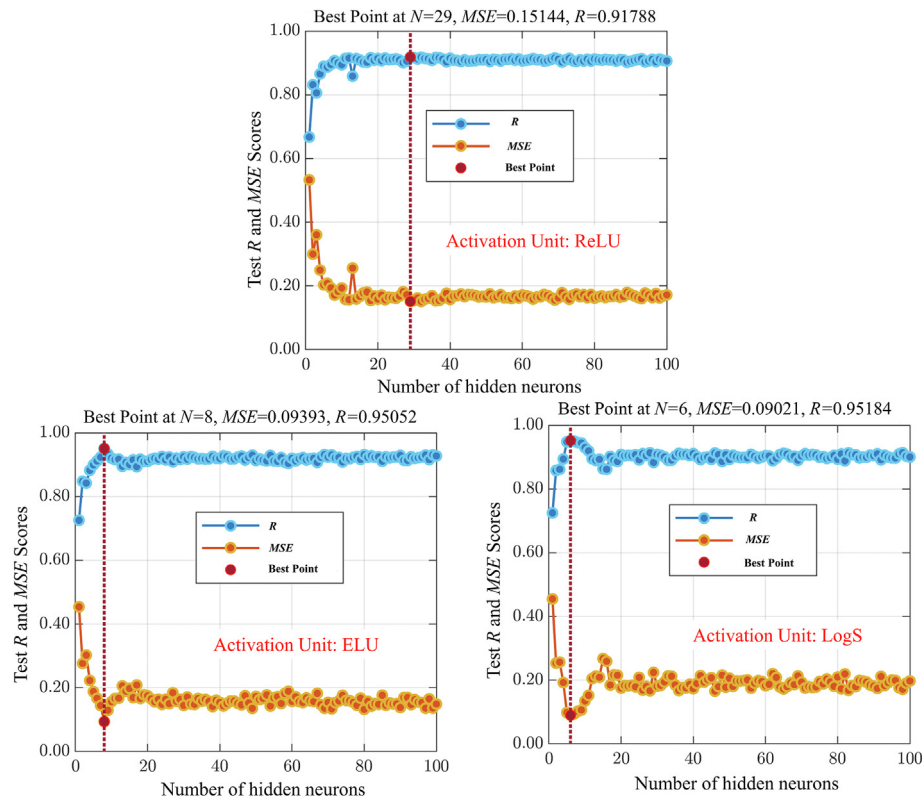


Fig. 12. Results of the grid search approach for each activation function considered.

the activation function. Since SNN-ReLU model does not consider the nonlinearity in the data training, the low fitting values were observed.

To verify that the SNN-LogS had returned a smooth regression of the data (without excessive oscillations, not physically acceptable), the three target variables were predicted, separately for the different proportions of PP, PA, curing period, curing method, and F-T cycles. The neural model developed can predict the performances of the stabilized expansive soil subgrades, by means of the numerical prediction, for a different composition of PA and PP, curing period, curing method, and F-T cycles, without the necessity to perform any other laboratory tests.

#### 4. Conclusions

The coupling effect of PA and PP fiber on strength and durability was explored in this study. A sustainable approach to control the behavior of the expansive soil subgrades by considering industrial waste was proposed. The various mechanical, chemical and microstructural tests were conducted to quantify the coupling effect of PA and PP fiber on expansive soil. The ANN model was also developed to predict the durability of the treated expansive soil to minimize extensive experimental work. The present study was conducted at the laboratory scale, and therefore, before implementing the optimum percentages of PA and PP fiber, large-scale field tests are required. Based on the detailed experimental and numerical investigations, the following conclusions are drawn:

- (1) The PA possesses the cement-like property and can be used as an alternative for the expansive soil stabilization as a sustainable approach. Addition of PA shows the densified soil-PP fiber matrix. The formation of the CSH gel also reduces the cavity in the expansive soil.

- (2) The WS and MC are effective curing methods and should be used for the treatment. The effect of GB curing is minimal and can be avoided for the curing method.
- (3) The inclusion of PA shows higher UCS and UPV values. However, very less STS is observed. The coupling effect of PA and PP shows an exponential increment in UCS, UPV and STS.
- (4) The inert nature of PP fiber under F-T cycles shows the higher durability of PP fiber-reinforced expansive soil and minimal strength loss. However, PA-stabilized samples undergo higher strength loss during F-T cycles due to nonrecurring volume change.
- (5) The detailed experimental analysis shows that the combination of 20% PA and 0.5% PP fiber is highly effective for the treatment of expansive soil and can be considered as the optimum proportion.
- (6) As for the future development of the modeling procedure, it is suggested that the adoption of an optimization technique for the selection of the ANN structure to reduce computational time, such as Bayesian statistics. The correlation coefficient ( $R$ ) approaches up to 0.95184.

#### Declaration of competing interest

The authors wish to confirm that there are no known conflicts of interest associated with this publication and there has been no significant financial support for this work that could have influenced its outcome.

#### Acknowledgments

We are grateful to Sophisticated Instrumentation Centre (SIC), Indian Institute of Technology Indore for providing material characterization facility. The authors would also acknowledge the

support of Ministry of Education, the Government of India, for funding the PhD Scholarship of the first author Mr. Nitin Tiwari.

## References

- Al-Rawas, A.A., Hago, A.W., Al-Sarmi, H., 2005. Effect of lime, cement and Sarooj (artificial pozzolan) on the swelling potential of an expansive soil from Oman. *Build. Environ.* 40 (5), 681–687.
- Behnood, A., 2018. Soil and clay stabilization with calcium- and non-calcium-based additives: a state-of-the-art review of challenges, approaches and techniques. *Transp. Geotech.* 17, 14–32.
- Bhurte, A., Eisazadeh, A., 2020. Strength and durability of bottom ash and lime stabilized Bangkok clay. *KSCSE J. Civ. Eng.* 24 (2), 404–411.
- Bilondi, M.P., Toufigh, M.M., Toufigh, V., 2018. Using calcium carbide residue as an alkaline activator for glass powder–clay geopolymer. *Construct. Build. Mater.* 183, 417–428.
- Bouziadi, F., Boulekache, B., Hamrat, M., 2016. The effects of fibres on the shrinkage of high-strength concrete under various curing temperatures. *Construct. Build. Mater.* 114, 40–48.
- Camargo, F.F., Edil, T.B., Benson, C.H., 2013. Strength and stiffness of recycled materials stabilised with fly ash: a laboratory study. *Road Mater. Pavement Des.* 14 (3), 504–517.
- Canakci, H., Güllü, H., Alhashemy, A., 2019. Performances of using geopolymers made with various stabilizers for deep mixing. *Materials* 12 (16), 2542.
- Chauhan, M.S., Mittal, S., Mohanty, B., 2008. Performance evaluation of silty sand subgrade reinforced with fly ash and fibre. *Geotext. Geomembranes* 26 (5), 429–435.
- Ding, L.Q., Han, Z., Zou, W.L., Wang, X.Q., 2020. Characterizing hydro-mechanical behaviours of compacted subgrade soils considering effects of freeze-thaw cycles. *Transp. Geotech.* 24, 100392.
- Du, C.X., Yang, G., Zhang, T.T., Yan, G.Q., 2019. Multiscale study of the influence of promoters on low-plasticity clay stabilized with cement-based composites. *Construct. Build. Mater.* 213, 537–548.
- García-Lodeiro, I., Fernández-Jimenez, A., Palomo, A., Macphee, D.E., 2010. Effect on fresh C-S-H gels of the simultaneous addition of alkali and aluminium. *Cement Concr. Res.* 40 (1), 27–32.
- Goodarzi, A.R., Akbari, H.R., Salimi, M., 2016. Enhanced stabilization of highly expansive clays by mixing cement and silica fume. *Appl. Clay Sci.* 132–133, 675–684.
- Ikeagwuani, C.C., Nwonu, D.C., 2019. Emerging trends in expansive soil stabilization: a review. *J. Rock Mech. Geotech. Eng.* 11 (2), 423–440.
- Inkoom, S., Sobanjo, J., Barbu, A., Niu, X.F., 2019. Prediction of the crack condition of highway pavements using machine learning models. *Struct. and Infra. Eng.* 15 (7), 940–953.
- IS 10082, 1981. Method of Test for Determination of Tensile Strength by Indirect Tests on Rock Specimens. Bureau of Indian Standards, India.
- IS 2720-1, 1983. Methods of Test for Soils, Preparation of Dry Soil Samples for Various Tests. Bureau of Indian Standards, India.
- IS 2720-10, 1991. Methods of Test for Soils, Determination of Unconfined Compressive Strength. Bureau of Indian Standards, India.
- IS 2720-3, 1980. Methods of Test for Soils, Determination of Specific Gravity, Section 1 Fine Grained Soils. Bureau of Indian Standards, India.
- IS 2720-4, 1985. Methods of Test for Soils, Grain Size Analysis. Bureau of Indian Standards, India.
- IS 2720-40, 1977. Methods of Test for Soils, Determination of Free Swell Index of Soils. Bureau of Indian Standards, India.
- IS 2720-5, 1985. Methods of Test for Soils, Determination of Liquid and Plastic Limit. Bureau of Indian Standards, India.
- IS 2720-7, 1980. Methods of Test for Soils, Determination of Water Content-Dry Density Relation Using Light Compaction. Bureau of Indian Standards, India.
- Kalinkin, A.M., Kalinkina, E.V., Politov, A.A., Makarov, V.N., Boldyrev, V.V., 2004. Mechanochemical interaction of Ca silicate and aluminosilicate minerals with carbon dioxide. *J. Mater. Sci.* 39, 5393–5398.
- Khazaei, J., Moayedi, H., 2019. Soft expansive soil improvement by eco-friendly waste and quick lime. *Arabian J. Sci. Eng.* 44, 8337–8346.
- Li, M., He, H., Senetakis, K., 2017. Behavior of carbon fiber-reinforced recycled concrete aggregate. *Geosynth. Int.* 24 (5), 480–490.
- Liu, Y.Y., Su, Y.H., Namdar, A., Zhou, G.Q., She, Y.X., Yang, Q., 2019. Utilization of cementitious material from residual rice husk ash and lime in stabilization of expansive soil. *Adv. Civ. Eng.* 2, 1–17.
- Lu, Y., Liu, S.H., Weng, L.P., Wang, L.J., Li, Z., Xu, L., 2016. Fractal analysis of cracking in a clayey soil under freeze-thaw cycles. *Eng. Geol.* 208, 93–109.
- Lu, Y., Liu, S.H., Alonso, E., Wang, L.J., Xu, L., Li, Z., 2019. Volume changes and mechanical degradation of a compacted expansive soil under freeze-thaw cycles. *Cold Reg. Sci. Technol.* 157, 206–214.
- MacKay, D.J.C., 1992. Bayesian interpolation. *Neural Comput.* 4 (3), 415–447.
- Moayedi, H., Nazir, R., 2018. Malaysian experiences of peat stabilization, state of the art. *Geotech. Geol. Eng.* 36, 1–11.
- Moghal, A.A.B., Chittoori, B.C.S., Basha, B.M., 2018. Effect of fibre reinforcement on CBR behaviour of lime-blended expansive soils: reliability approach. *Road Mater. Pavement Des.* 19 (3), 690–709.
- Paykov, O., Hawley, H., 2015. Property-based assessment of soil mineralogy using mineralogy charts. *Appl. Clay Sci.* 104, 261–268.
- Prasannan, S., Kolathayar, S., Sharma, A.K., 2020. Comparative study on bearing capacity of bottom ash–stabilized soil mixed with natural and synthetic fibers. *Adv. Civ. Eng. Mater.* 9 (1), 411–426.
- Puppala, A.J., Pedarla, A., Pino, A., Hoyos, L.R., 2017. Diffused double-layer swell prediction model to better characterize natural expansive clays. *J. Eng. Mech.* 143 (9), 04017069.
- Rojas, E., Romo, M.P., Cervantes, R., 2009. Closure to “analysis of deep moisture barriers in expansive soils. I: constitutive model formulation” by Eduardo Rojas, Miguel P. Romo, and Refugio Cervantes. *Int. J. GeoMech.* 9 (2), 87–88.
- Sharma, L.K., Sirdesai, N.N., Sharma, K.M., Singh, T.N., 2018. Experimental study to examine the independent roles of lime and cement on the stabilization of a mountain soil: a comparative study. *Appl. Clay Sci.* 152, 183–195.
- Sharma, M., Satyam, N., Reddy, K.R., 2019. Investigation of various gram-positive bacteria for MICP in Narmada Sand, India. *Int. J. Geotech. Eng.* 15 (2), 220–234.
- Shi, B., Wu, Z., Inyang, H., Chen, J., Wang, B., 1999. Preparation of soil specimens for SEM analysis using freeze-cut-drying. *Bull. Eng. Geol. Environ.* 58 (1), 1–7.
- Singh, S.P., Rout, S., Tiwari, A., 2018. Quantification of desiccation cracks using image analysis technique. *Int. J. Geotech. Eng.* 12 (4), 383–388.
- Soundara, B., Robinson, R.G., 2009. Influence of test method on swelling pressure of compacted clay. *Int. J. Geotech. Eng.* 3 (3), 439–444.
- Steinberg, M., 1998. *Geomembranes and the Control of Expansive Soils in Construction*. McGraw-Hill, New York, NY, US.
- Sudhakaran, S.P., Sharma, A.K., Kolathayar, S., 2018. Soil stabilization using bottom ash and areca fiber: experimental investigations and reliability analysis. *J. Mater. Civ. Eng.* 30 (8), 04018169.
- Tataranni, P., Sangiorgi, C., Simone, A., Vignali, V., Lantieri, C., Dondi, G., 2018. A laboratory and field study on 100% recycled cement bound mixture for base layers. *Int. J. Pavement Res. Technol.* 11 (5), 427–434.
- Tiwari, N., Satyam, N., 2019. Experimental study on the influence of polypropylene fiber on the swelling pressure expansion attributes of silica fume stabilized clayey soil. *Geosciences* 9 (9), 377.
- Temuujin, J., Riessen, A.V., Williams, R., 2009. Influence of calcium compounds on the mechanical properties of fly ash geopolymer pastes. *J. Hazard Mater.* 167 (1–3), 82–88.
- Tiwari, N., Satyam, N., 2020. An experimental study on the behavior of lime and silica fume treated coir geotextile reinforced expansive soil subgrade. *Eng. Sci. Technol. an Int. J.* 23 (5), 1214–1222.
- Tiwari, N., Satyam, N., Patva, J., 2020a. Engineering characteristics and performance of polypropylene fibre and silica fume treated expansive soil subgrade. *Int. J. Geosynth. Gr. Eng.* 6 (2), 1–11.
- Tiwari, N., Satyam, N., Singh, K., 2020b. Effect of curing on micro-physical performance of polypropylene fiber reinforced and silica fume stabilized expansive soil under freezing thawing cycles. *Sci. Rep.* 10 (1), 7624.
- Tiwari, N., Satyam, N., Shukla, S.K., 2020c. An experimental study on micro-structural and geotechnical characteristics of expansive clay mixed with EPS granules. *Soils Found.* 60 (3), 705–713.
- Tiwari, N., Satyam, N., Puppala, A.J., 2021. Strength and durability assessment of expansive soil stabilized with recycled ash and natural fibers. *Transp. Geotech.* 29, 100556.
- Tizpa, P., Chenari, R.J., Fard, M.K., s Machado, S.L., 2015. ANN prediction of some geotechnical properties of soil from their index parameters. *Arab. J. Geosciences.* 8 (5), 2911–2920.
- Wilberforce, T., Baroutaji, A., Soudan, B., Al-Alami, A.H., Olabi, A.G., 2019. Outlook of carbon capture technology and challenges. *Sci. Total Environ.* 657, 56–72.
- Wong, L.C., Haug, M., 1991. Cyclical closed-system freeze–thaw permeability testing of soil liner and cover materials. *Can. Geotech. J.* 28 (6), 784–793.
- Zhang, M., Zhao, M.X., Zhang, G.P., Nowak, P., Coen, A., Tao, M.J., 2015. Calcium-free geopolymer as a stabilizer for sulfate-rich soils. *Appl. Clay Sci.* 108, 199–207.



**Nitin Tiwari** obtained his BE and ME degrees from Rajiv Gandhi Technical University Bhopal, India. He is pursuing a PhD from the Indian Institute of Technology Indore, India, and receiving a Teaching Assistantship (TA) fellowship from the Ministry of Education, India. He is actively engaged in teaching, research, and consultancy in the field of civil engineering, particularly in geotechnical engineering and pavement engineering. He is an expert in machine learning and artificial intelligence application in civil engineering. He majorly works on sustainable materials for pavements. He has been authored more than 10 scientific papers. He is a member of several professional societies such as a lifetime member of the International Geosynthetic Society (IGS), lifetime member of the Indian Geotechnical Society (IGS), member of the International Association of Engineers (IAENG), member of the American Concrete Institute (ACI), member of National Society of Professional Engineers (NSPE), and member of the Institution of Structural Engineers (ISE). In recent years, he has been awarded the Young Scientist Award (2021) by the Madhya Pradesh Council of Science and Technology Bhopal, India.